



Sequence Isomeric Giant Surfactants with Distinct Self-Assembly in Solution

Journal:	<i>ChemComm</i>
Manuscript ID	CC-COM-11-2018-009207.R1
Article Type:	Communication

SCHOLARONE™
Manuscripts



6 Sequence Isomeric Giant Surfactants with Distinct Self-Assembly 7 in Solution

1 Received 00th January 20xx, 8 Wei Zhang,^a Wenpeng Shan,^a Shuailin Zhang,^a Yuchu Liu,^a Hao Su,^b Jiancheng Luo,^a Yanfeng Xia,^a
2 Accepted 00th January 20xx 9 Tao, Li,^c Chrys Wesdemiotis,^{a,d} Tianbo Liu,^a Honggang Cui,^b Yiwen Li,^{e*} Stephen Z.D. Cheng^{a,f*}

3 DOI: 10.1039/x0xx00000x

4 www.rsc.org/

10 We have designed and synthesized a pair of sequence isomeric
11 giant surfactants based on polystyrene (PS) and polyhedral
12 oligomeric silsesquioxane (POSS) nanoparticles. Although those
13 two macromolecules possess identical compositions as “sequence
14 isomers”, the distinctly arranged POSS sequence leads to different
15 molecular packing conformation, and further induce distinguished
16 self-assembly behaviors in DMF/water solutions.

17 Design and synthesis of sequence-defined macromolecules has
18 attracted a lot of attentions in recent years and still remains to be
19 very challenging. In the synthetic aspect, quite a few elegant
20 approaches have been developed.¹⁻⁹ For instance, Meier et al.
21 developed a method to synthesize sequence-controlled oligomers
22 through the Passerini three-component reaction.¹⁰ Lutz and
23 workers synthesized sequence-coded polymers with >10k Dalton
24 molecular masses based on the phosphoramidite coupling
25 reaction.^{11,12} Zhang’s group achieved sequence-controlled polymers
26 by using furan-protected maleimide as a latent monomer.¹³ Although
27 sequence has been well known to be one of the key molecular
28 parameters to determine the structures and properties of
29 biomacromolecules, such as peptides, peptoids and nucleic acid,¹⁴⁻¹⁸
30 there are only limited amount of works regarding to the sequence
31 effect on synthetic macromolecules.¹⁹⁻²² Johnson et al. very recently
32 demonstrated that the stereochemical sequence could dictate
33 unimolecular diblock copolymer assembly in the bulk.²³ Our group
34 has developed sequence-controlled “giant molecules”, which are

precisely defined macromolecules in terms of stereochemistry,
composition, sequence, topology and molecular mass built on
molecular nanoparticles (MNP) such as polyhedral oligomeric
silsesquioxane (POSS) nanoparticles.²⁴⁻²⁶ By using POSS nanoparticles
as macromonomers, the sequence effect of giant molecules can be
amplified, and versatile distinct phase structures, including
unconventional Frank-Kasper A15, sigma and dodecagonal
quasicrystal structures, have been obtained from the sequence
isomers in the solid state.^{24, 27} It could also be interesting to
investigate the sequence effect of synthetic macromolecules on their
self-assembly behaviors in solution or thin film states.

In another aspect, the solution self-assembly behaviors of giant
surfactants have been widely investigated in our group.²⁸⁻³⁰ Giant
surfactants are a kind of precisely defined amphiphilic
macromolecules composed of MNP heads and polymer tails. These
giant surfactants capture the essential feature of small molecular
surfactants while possess much larger sizes.²⁸ They are thus bridging
the gap between traditional amphiphilic block copolymers and small
molecular surfactants. Several macromolecular parameters, such as
the molecular composition and topology, have been demonstrated
to play important roles in the self-assemble behaviors of giant
surfactants in solution.³⁰⁻³³ To further advance our understanding,
how does the sequence, as another molecular parameter, affect the
solution assembly of giant surfactants remains to be explored. In this
letter, we have prepared a pair of polystyrene (PS) and POSS-based
“sequence isomers” PS-(BPOSS)₂(APOSS) and PS-(APOSS)(BPOSS)₂
(denoted as PS-BBA and PS-ABB, where B represents BPOSS with
seven isobutyl groups at corners of the POSS core, and A represents
APOSS with seven carboxylic acid groups at corners of the POSS core)
to explore the effect of sequence in giant surfactants.

^a Department of Polymer Science, College of Polymer Science and Polymer Engineering, The University of Akron, Akron, Ohio, 44325-3909, United States

^b Department of Chemical and Biomolecular Engineering, The Johns Hopkins University, Baltimore, MD 21218, United States

^c Department of Chemistry, The University of Akron, Akron, Ohio 44325-3601, United States

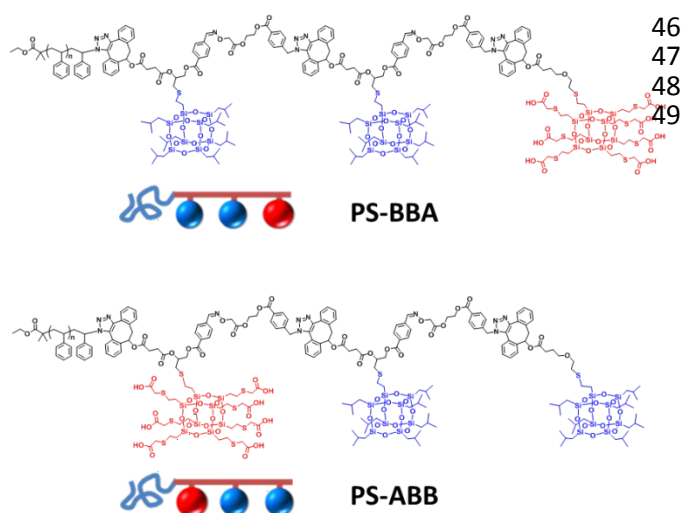
^d X-ray Science Division, Advanced Photon Source, Argonne National Laboratory, Argonne, Illinois, 60439, United States; Department of Chemistry and Biochemistry Northern Illinois University, DeKalb, IL 60115, United States

^e College of Polymer Science and Engineering, State Key Laboratory of Polymer Materials Engineering, Sichuan University, Chengdu, 610065, China

^f South China Advanced Institute for Soft Matter Science and Technology, South China University of Technology, Guangzhou, China, 510640

† Footnotes relating to the title and/or authors should appear here.

Electronic Supplementary Information (ESI) available: [details of any supplementary information available should be included here]. See DOI: 10.1039/x0xx00000x

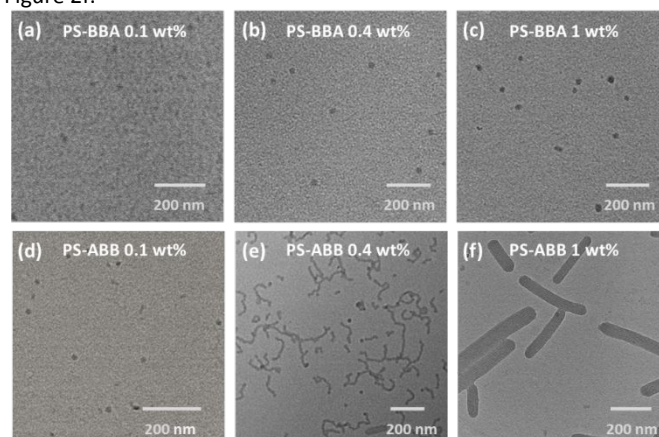


1
2 Figure 1. Molecular structures of PS-ABB and PS-BBA.

3
4 The polymer-POSS conjugates are synthesized through
5 iteratively performed strain-promoted alkyne cycloadditions (SPAAC)
6 and oxime ligations as we previously reported.⁸ Their molecular
7 structures are shown in Figure 1. The detailed synthetic route is listed
8 in the Supporting Information. The building blocks such as DIBO-B-
9 CHO, DIBO-V-CHO, DIBO-B, DIBO-V and the “click adaptor” were
10 prepared as previously described.^{8, 27} An azido terminated
11 polystyrene (PS-N₃) with molecular weight of 2k is used as the
12 starting material. Then, two BPOSSs are installed onto the polymer
13 chain-end through two reaction cycles of SPAAC and oxime ligations,
14 followed by attaching one more VPOSS, which has seven vinyl groups
15 at each corner and is the precursor of APOSS. As the POSS NPs are
16 attached onto the polymer chains, in the ¹H NMR spectra, the
17 characteristic signals from BPOSS (δ 1.8-1.9 ppm for $-\text{CH}(\text{CH}_3)_2$) and
18 VPOSS (δ 5.8-6.2 ppm for $-\text{CH}=\text{CH}_2$) appear clearly as shown in Figure
19 S1a, and the GPC curves exhibit clear shift toward low retention time,
20 indicating the increase of molecular weight (Figure S1b).
21 Furthermore, matrix-assisted laser desorption ionization time-of-
22 flight (MALDI-TOF) mass spectrum also shows consistent molecular
23 weight compared to the calculated molecular weight with a single
24 distribution with distance of 104 Da., which corresponds to a styrene
25 repeat unit (Figure S1c). Finally, VPOSS is converted into APOSS via
26 thiol-ene click reaction³⁴ to afford PS-BBA (Scheme S2). Its “sequence
27 isomer” PS-ABB can be synthesized in a similar way but just with the
28 incorporation of VPOSS or BPOSS in a different step (Scheme S3). Due
29 to the same chemical composition, these two macromolecules show
30 almost identical NMR, GPC and MALDI-TOF spectra (Figures S2-S5).

31 In the solution assembly study, dimethylformamide (DMF) was
32 used as the common solvent for both the hydrophilic and
33 hydrophobic parts to dissolve the materials at different initial
34 concentrations, water was then added very slowly into the system
35 as we previously described for PS-(APOSS)_n samples.^{29, 31} In order to
36 directly compare the influence of sequence issue on these two giant
37 molecules, we used exactly identical conditions to prepare the
38 micellar samples, including initial concentrations of 0.1 wt%, 0.4 wt%
39 and 1 wt%, respectively. It was observed in the transmission electron
40 microscopy (TEM) results that PS-BBA can only form spherical
41 aggregates at different initial concentrations in the experiment
42 (Figures 2a-2c). However, it is very interesting to note that the
43 “sequence isomer” PS-ABB shows different assembly morphologies.
44 For example, at a low concentration (0.1 wt%), it also forms spherical
45 assemblies (Figure 2d). As the initial concentration increases to 0.4

wt%, it becomes cylindrical assemblies (Figure 2e). Further increase
the initial concentration to 1 wt%, it could form a kind of ribbon-like
assemblies instead of traditional vesicular structures as show in
Figure 2f.



50
51
52
53
54
55
56
57
58
59
60
61
62
63
64
65
66
67
68
69
70
71
72
73
74
75
76
77
78
79
80
81
82
83
84
85
86
87
88
89
90
91
92
93
94
95
96
97
98
99
100
101
102
103
104
105
106
107
108
109
110
111
112
113
114
115
116
117
118
119
120
121
122
123
124
125
126
127
128
129
130
131
132
133
134
135
136
137
138
139
140
141
142
143
144
145
146
147
148
149
150
151
152
153
154
155
156
157
158
159
160
161
162
163
164
165
166
167
168
169
170
171
172
173
174
175
176
177
178
179
180
181
182
183
184
185
186
187
188
189
190
191
192
193
194
195
196
197
198
199
200
201
202
203
204
205
206
207
208
209
210
211
212
213
214
215
216
217
218
219
220
221
222
223
224
225
226
227
228
229
230
231
232
233
234
235
236
237
238
239
240
241
242
243
244
245
246
247
248
249
250
251
252
253
254
255
256
257
258
259
260
261
262
263
264
265
266
267
268
269
270
271
272
273
274
275
276
277
278
279
280
281
282
283
284
285
286
287
288
289
290
291
292
293
294
295
296
297
298
299
300
301
302
303
304
305
306
307
308
309
310
311
312
313
314
315
316
317
318
319
320
321
322
323
324
325
326
327
328
329
330
331
332
333
334
335
336
337
338
339
340
341
342
343
344
345
346
347
348
349
350
351
352
353
354
355
356
357
358
359
360
361
362
363
364
365
366
367
368
369
370
371
372
373
374
375
376
377
378
379
380
381
382
383
384
385
386
387
388
389
390
391
392
393
394
395
396
397
398
399
400
401
402
403
404
405
406
407
408
409
410
411
412
413
414
415
416
417
418
419
420
421
422
423
424
425
426
427
428
429
430
431
432
433
434
435
436
437
438
439
440
441
442
443
444
445
446
447
448
449
450
451
452
453
454
455
456
457
458
459
460
461
462
463
464
465
466
467
468
469
470
471
472
473
474
475
476
477
478
479
480
481
482
483
484
485
486
487
488
489
490
491
492
493
494
495
496
497
498
499
500
501
502
503
504
505
506
507
508
509
510
511
512
513
514
515
516
517
518
519
520
521
522
523
524
525
526
527
528
529
530
531
532
533
534
535
536
537
538
539
540
541
542
543
544
545
546
547
548
549
550
551
552
553
554
555
556
557
558
559
560
561
562
563
564
565
566
567
568
569
570
571
572
573
574
575
576
577
578
579
580
581
582
583
584
585
586
587
588
589
590
591
592
593
594
595
596
597
598
599
600
601
602
603
604
605
606
607
608
609
610
611
612
613
614
615
616
617
618
619
620
621
622
623
624
625
626
627
628
629
630
631
632
633
634
635
636
637
638
639
640
641
642
643
644
645
646
647
648
649
650
651
652
653
654
655
656
657
658
659
660
661
662
663
664
665
666
667
668
669
670
671
672
673
674
675
676
677
678
679
680
681
682
683
684
685
686
687
688
689
690
691
692
693
694
695
696
697
698
699
700
701
702
703
704
705
706
707
708
709
710
711
712
713
714
715
716
717
718
719
720
721
722
723
724
725
726
727
728
729
730
731
732
733
734
735
736
737
738
739
740
741
742
743
744
745
746
747
748
749
750
751
752
753
754
755
756
757
758
759
760
761
762
763
764
765
766
767
768
769
770
771
772
773
774
775
776
777
778
779
780
781
782
783
784
785
786
787
788
789
790
791
792
793
794
795
796
797
798
799
800
801
802
803
804
805
806
807
808
809
810
811
812
813
814
815
816
817
818
819
820
821
822
823
824
825
826
827
828
829
830
831
832
833
834
835
836
837
838
839
840
841
842
843
844
845
846
847
848
849
850
851
852
853
854
855
856
857
858
859
860
861
862
863
864
865
866
867
868
869
870
871
872
873
874
875
876
877
878
879
880
881
882
883
884
885
886
887
888
889
890
891
892
893
894
895
896
897
898
899
900
901
902
903
904
905
906
907
908
909
910
911
912
913
914
915
916
917
918
919
920
921
922
923
924
925
926
927
928
929
930
931
932
933
934
935
936
937
938
939
940
941
942
943
944
945
946
947
948
949
950
951
952
953
954
955
956
957
958
959
960
961
962
963
964
965
966
967
968
969
970
971
972
973
974
975
976
977
978
979
980
981
982
983
984
985
986
987
988
989
990
991
992
993
994
995
996
997
998
999
1000

Figure 2. TEM images of the assembled structures of PS-BBA (a-c) and PS-ABB (d-f) at initial concentration of 0.1 wt%, 0.4 wt% and 1 wt%, respectively.

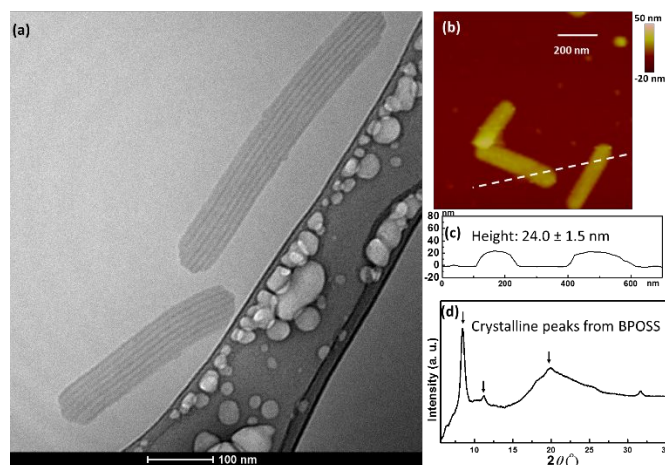


Figure 3. Characterizations of the ribbon-like structure of PS-ABB. (a) cryo-TEM image; (b) AFM image and (c) height profile (d) wide angle X-ray diffraction.

By looking at the ribbon-like assemblies in details, phase separated lamellar structures exist with spacing of about 10 nm. The ribbon-like structure is further confirmed by Cryo-TEM to exclude the drying effects (Figure 3a). The lengths of the ribbon-like assemblies are several hundreds of nanometers with widths around 70-100 nm from the TEM results. The thickness of the ribbon-like assemblies is measured to be about 25 nm using atomic force microscope (AFM) (Figures 3b and 3c).

The concept of packing parameter (p) established in self-assembly of small molecular surfactant system also can be applied to evaluate giant surfactants.²⁹⁻³¹ It is defined as $p = V/(a \times l)$, where V , l and a are the volume and length of the hydrophobic tail, and the cross-section area of the hydrophilic head group, respectively.³⁵ Three regions of the p values, $p < 0.33$, $0.33 < p < 0.5$, and $p > 0.5$, usually indicate spherical micelles, cylindrical micelles and vesicles/lamellae, respectively. Our previous work has demonstrated that the initial concentration of giant surfactant is one of the criteria in determining the final assembled structure via the degree of ionization of carboxylic acid groups on APOSS, which decreases as

the initial concentration increases.³⁰ This results in the reduction of effective head size and cross-section area of the surfactant, finally leading to the increase of p .³¹

For these two sequence isomeric giant surfactants, the volume of the hydrophobic part (V) is identical and can be estimated to 5.6 nm^3 by the following calculation:

$$V = V_B + V_{PS} = \frac{M_B}{N_{APB}} + \frac{M_{PS}}{N_{APPS}},$$

where V_B and V_{PS} are the volume of the BPOSS and PS parts respectively; $M_B = 1.6 \text{ kg/mol}$ (for simplification we include the linker as well) and $M_{PS} = 2 \text{ kg/mol}$ are the molecular mass of the BPOSS and PS parts, respectively; $\rho_B = 1.1 \text{ g/cm}^3$ and $\rho_{PS} = 1.04 \text{ g/cm}^3$ are their densities;³⁶ and N_A is the Avogadro constant.

Polymer tails in giant surfactant has been previously found to be highly stretched especially for low molecular weight, which is different from most traditional amphiphilic block copolymers.²⁹ So for simplified qualitative analysis of the difference in self-assembly trending, the contour length of polystyrene tail (l_{PS}) in this work can be estimated about 5 nm by $l = 0.154n\sin(109.5^\circ/2)$, where $n = 40$ (two carbons per repeat unit). The length of BPOSS part with the linkers (l_B) is also about 5 nm . When we assume no ionization condition, the smallest cross-section area of APOSS (a_A) can be estimated to be 1.8 nm^2 according to its diameter of about 1.5 nm . In the self-assembly of PS-BBA, the hydrophobic BPOSS and PS are on the same side of APOSS and thus, they could stay together in the hydrophobic core. This molecule resembles a "one-head one-tail" giant surfactant. As the initial concentration increase, the degree of ionization of carboxylic acids on APOSS decreases, which leads in the decrease of effective head size and a_A ,³¹ so that p becomes larger. Note that p reaches the maximum possible value by assuming no ionization of APOSS and the polar head becomes the smallest volume. It could be calculated to be $p_{\max} \approx 0.31$ via the formula $p_{PS-BBA} = V/[a \times (l_{PS} + l_B)]$. Therefore, the macromolecule would only adapt to a cone-shape conformation and form spheres with any initial concentration of PS-BBA. At the same time, the cone-angle may decrease due to the smaller heads thus more molecules will assemble into one sphere as the concentration increases. This is evidenced from the light scattering experiments in Figure S5 that the size of the spheres increases with the initial concentrations. Notably, the assumption of using contour length of PS in the calculation is also supported by analyzing the spherical micelles of PS-BBA with initial concentration of 0.1% as an example. By subtracting the size of APOSS and the length of BPOSS part with linkers from the measured micelle size of about 11 nm , the calculated length of PS part is about 4.5 nm , which is closed to its fully stretched length.

While for the other sequence isomer PS-ABB, the hydrophobic PS and BPOSS are phase separated by APOSS. In order to avoid the hydrophobic moieties to direct contact with water, the molecule has to adapt to a folded conformation so that both the PS and BPOSS could stay in the hydrophobic core phase. This makes PS-ABB resemble a "one head two heterogeneous tails" giant surfactant, which one tail is PS and another tail is two BPOSSs. The two bulky "parallel" linked tails of PS-ABB will make its assembly behavior very different from its sequence isomer PS-BBA. The maximum possible value can be calculated to be $p_{\max} \approx 0.62$ based on the similar calculation (See SI). Therefore, PS-ABB has higher tendency to form non-spherical assemblies such as cylindrical micelles or vesicles especially at higher concentrations. When the concentration is relatively high at $1 \text{ wt}\%$, we speculate that $p > 0.5$ and the it should be in the "vesicle/lamellae region", in which giant surfactants usually forms vesicles.²⁸ However, in this case, the PS-ABB molecules alternatively form the nanoribbon-like assemblies containing

lamellar structure within the ribbons. It is known that BPOSS is a crystalline moiety.³⁷⁻³⁹ When the molecule is in or close to a "vesicle/lamellae region", crystallization with high enthalpy may act as the driving force to form unconventional structures.⁴⁰ In current case, we speculate that BPOSS may have crystallized, so that a straight lamellar structure is preferred instead of vesicles. According to literature and the above experiments, the freeze-dried self-assemblies of these giant surfactant in solution as shown in Figure 4a could represent their true solution state.²⁹ So, we perform wide angle X-ray diffraction (WAXD) of the freeze-dried PS-ABB assembled nanoribbon-like structure. In Figure 3d, it clearly shows the diffraction peaks attributed to crystalline BPOSS,^{38, 41} which supports our speculation. As the concentration decreases, a_A increases and p decreases. For $0.4 \text{ wt}\%$, p value may decrease to below 0.5 , thereby, worm-like cylindrical assemblies are observed. At the lowest concentration of 0.1% , p may further decrease to be below 0.33 , the assembled structures thus become spheres. In these two cases, due to the formation of curvature structures, BPOSSs are not crystallized, which is confirmed by the WAXD spectra of the corresponding freeze-dried samples as shown in Figure S9. Therefore, a possible model summary of the self-assembly behaviors of these two sequential isomers is proposed in Figure 4.

In addition to different self-assembly behaviors in solution, PS-ABB and PS-BBA also show differences in the bulk state. PS-ABB can also form a lamellar structure after thermal annealing (Figure S10a), but only a disorder structure can be observed in PS-BBA sample (Figure S10b).

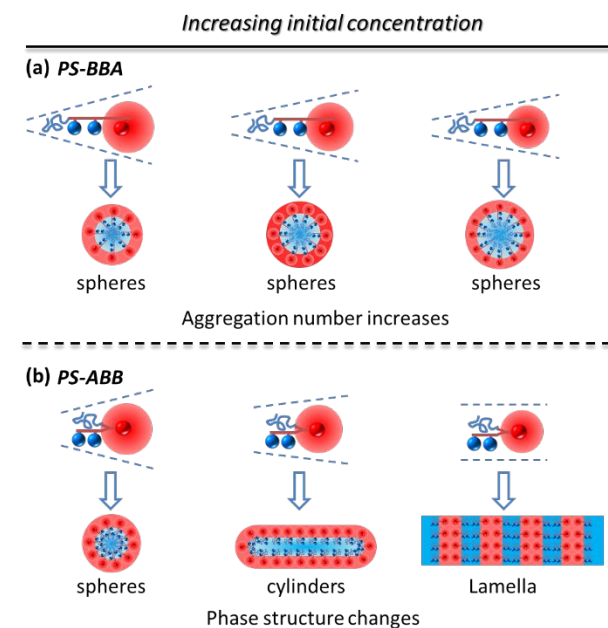


Figure 4. Proposed models for the illustration of the different assembly process for the sequential isomer: (a) PS-BBA and (b) PS-ABB. The blue ball represents BPOSS and the red ball represents APOSS. The red corona around the red ball indicates the partially ionized APOSS, which could become smaller when the initial concentration increases

To conclude, we have designed and synthesized two giant surfactants with exactly the same composition but different sequences, PS-ABB and PS-BBA. The distinct nanoparticle sequences in giant molecules could lead to different macromolecular conformations, which could further affect their separate self-assembly behaviors in DMF/water solution. The conjugate of PS-BBA, which resembles a "one head one tail" giant surfactant, can only

- 1 form spherical assemblies. While the conjugate of PS-ABB, which
 2 resembles a “one head two heterogeneous tail” giant surfactant, can
 3 form spheres, cylinders or a nanoribbon-like structure in response to
 4 different initial concentrations. With the growing field of sequence-
 5 controlled oligomer/polymer chemistry, these results further
 6 support the importance of sequence-control in synthesis of
 7 macromolecules, which can have dramatic impacts on the self-
 8 assembled structures and macromolecular properties. 65
- 9 This work was supported by NSF (DMR-1408872, CHE-1808116) and
 10 NSF (51603133). This research used resources of the Advanced
 11 Photon Source, a U.S. Department of Energy (DOE) Office of Science
 12 User Facility operated for the DOE Office of Science by Argonne
 13 National Laboratory under Contract No. DE-AC02-06CH11357. 70
- 14 **Conflicts of interest** 73
- 15 There are no conflicts to declare 74
- 16 **Notes and references** 78
- 17 1. M. L. McKee, P. J. Milnes, J. Bath, E. Stulz, A. J. Turberfield and
 18 R. K. O'Reilly, *Angew. Chem. Int. Ed.*, 2010, **49**, 7948-7951. 80
 - 19 2. M. Porel and C. A. Alabi, *J. Am. Chem. Soc.*, 2014, **136**, 13162-
 20 13165. 81
 - 21 3. Y.-H. Wu, J. Zhang, F.-S. Du and Z.-C. Li, *ACS Macro Lett.*, 2017,
 22 **6**, 1398-1403. 83
 - 23 4. A. Anastasaki, B. Oschmann, J. Willenbacher, A. Melker, M. H.
 24 Van Son, N. P. Truong, M. W. Schulze, E. H. Discekici, A. J.
 25 McGrath, T. P. Davis, C. M. Bates and C. J. Hawker, *Angew.*
 26 *Chem. Int. Ed.*, 2017, **56**, 14483-14487. 88
 - 27 5. S. Martens, J. Van den Begin, A. Madder, F. E. Du Prez and P.
 28 Espeel, *J. Am. Chem. Soc.*, 2016, **138**, 14182-14185. 90
 - 29 6. Y. Hibi, M. Ouchi and M. Sawamoto, *Nat. Commun.*, 2016, **7**,
 30 11064. 91
 - 31 7. W. Xi, S. Pattanayak, C. Wang, B. Fairbanks, T. Gong, J. Wagner,
 32 C. J. Kloxin and C. N. Bowman, *Angew. Chem. Int. Ed.*, 2015, **54**,
 33 14462-14467. 95
 - 34 8. W. Zhang, M. Huang, H. Su, S. Zhang, K. Yue, X.-H. Dong, X. Li,
 35 Liu, S. Zhang, C. Wesdemiotis, B. Lotz, W.-B. Zhang, Y. Li and S.
 36 Z. D. Cheng, *ACS Cent. Sci.*, 2016, **2**, 48-54. 98
 - 37 9. D. Debnath, J. A. Baughman, S. Datta, R. A. Weiss and C. Pugh,
 38 *Macromolecules*, 2018, **51**, 7951-7963. 100
 - 39 10. S. C. Solleder and M. A. R. Meier, *Angew. Chem. Int. Ed.*, 2014,
 40 **53**, 711-714. 102
 - 41 11. A. Al Ouahabi, L. Charles and J.-F. Lutz, *J. Am. Chem. Soc.*, 2015,
 42 **137**, 5629-5635. 103
 - 43 12. A. A. Ouahabi, M. Kotera, L. Charles and J.-F. Lutz, *ACS Macro*
 44 *Let.*, 2015, 1077-1080. 106
 - 45 13. Y. Ji, L. Zhang, X. Gu, W. Zhang, N. Zhou, Z. Zhang and X. Zhu,
 46 *Angew. Chem. Int. Ed.*, 2017, **56**, 2328-2333. 108
 - 47 14. J.-F. Lutz, M. Ouchi, D. R. Liu and M. Sawamoto, *Science*, 2013,
 48 **341**, 1238149. 110
 - 49 15. J. Sun, A. A. Teran, X. Liao, N. P. Balsara and R. N. Zuckerman,
 50 *J. Am. Chem. Soc.*, 2013, **135**, 14119-14124. 112
 - 51 16. C. Leng, H. G. Buss, R. A. Segalman and Z. Chen, *Langmuir*, 2015,
 52 **31**, 9306-9311. 114
 - 53 17. Y. Suzuki, G. Cardone, D. Restrepo, P. D. Zavattieri, T. S. Baker
 54 and F. A. Tezcan, *Nature*, 2016, **533**, 369-373. 115
 - 55 18. R. V. Thaner, Y. Kim, T. I. N. G. Li, R. J. Macfarlane, S. T. Nguyen,
 56 M. Olvera de la Cruz and C. A. Mirkin, *Nano Lett.*, 2015, **15**,
 57 5545-5551. 117
 19. C. Laure, D. Karamessini, O. Milenkovic, L. Charles and J.-F. Lutz,
Angew. Chem. Int. Ed., 2016, **55**, 10722-10725.
 20. J.-F. Lutz, J.-M. Lehn, E. W. Meijer and K. Matyjaszewski, *Nat.*
Rev. Mater., 2016, **1**, 16024.
 21. M. Porel, D. N. Thornlow, N. N. Phan and C. A. Alabi, *Nat.*
Chem., 2016, **8**, 590-596.
 22. J. Li, R. M. Stayshich and T. Y. Meyer, *J. Am. Chem. Soc.*, 2011,
133, 6910-6913.
 23. M. R. Golder, Y. Jiang, P. E. Teichen, H. V. T. Nguyen, W. Wang,
N. Milos, S. A. Freedman, A. P. Willard and J. A. Johnson, *J. Am.*
Chem. Soc., 2018, **140**, 1596-1599.
 24. W. Zhang, X. Lu, J. Mao, C.-H. Hsu, G. Mu, M. Huang, Q. Guo, H.
Liu, C. Wesdemiotis, T. Li, W.-B. Zhang, Y. Li and S. Z. D. Cheng,
Angew. Chem. Int. Ed., 2017, **56**, 15014-15019.
 25. W.-B. Zhang, X. Yu, C.-L. Wang, H.-J. Sun, I. F. Hsieh, Y. Li, X.-H.
Dong, K. Yue, R. Van Horn and S. Z. D. Cheng, *Macromolecules*,
2014, **47**, 1221-1239.
 26. K. Yue, M. Huang, R. L. Marson, J. He, J. Huang, Z. Zhou, J. Wang,
C. Liu, X. Yan, K. Wu, Z. Guo, H. Liu, W. Zhang, P. Ni, C.
Wesdemiotis, W.-B. Zhang, S. C. Glotzer and S. Z. D. Cheng,
Proc. Natl. Acad. Sci. U.S.A., 2016, **113**, 14195-14200.
 27. W. Zhang, S. Zhang, Q. Guo, X. Lu, Y. Liu, J. Mao, C.
Wesdemiotis, T. Li, Y. Li and S. Z. D. Cheng, *ACS Macro Lett.*,
2018, **7**, 635-640.
 28. X. Yu, Y. Li, X.-H. Dong, K. Yue, Z. Lin, X. Feng, M. Huang, W.-B.
Zhang and S. Z. D. Cheng, *J. Polym. Sci., Part B: Polym. Phys.*,
2014, **52**, 1309-1325.
 29. X. Yu, S. Zhong, X. Li, Y. Tu, S. Yang, R. M. Van Horn, C. Ni, D. J.
Pochan, R. P. Quirk, C. Wesdemiotis, W.-B. Zhang and S. Z. D.
Cheng, *J. Am. Chem. Soc.*, 2010, **132**, 16741-16744.
 30. X. Yu, W.-B. Zhang, K. Yue, X. Li, H. Liu, Y. Xin, C.-L. Wang, C.
Wesdemiotis and S. Z. D. Cheng, *J. Am. Chem. Soc.*, 2012, **134**,
7780-7787.
 31. Y. Chu, W. Zhang, X. Lu, G. Mu, B. Zhang, Y. Li, S. Z. D. Cheng and
T. Liu, *Chem. Commun.*, 2016, **52**, 8687-8690.
 32. W. Zhang, Y. Chu, G. Mu, S. A. Eghtesadi, Y. Liu, Z. Zhou, X. Lu,
M. A. Kashfipour, R. S. Lillard, K. Yue, T. Liu and S. Z. D. Cheng,
Macromolecules, 2017, **50**, 5042-5050.
 33. S. A. Eghtesadi, M. A. Kashfipour, X. Sun, W. Zhang, R. S. Lillard,
S. Z. D. Cheng and T. Liu, *Nanoscale*, 2018, **10**, 1411-1419.
 34. Y. Li, X.-H. Dong, Y. Zou, Z. Wang, K. Yue, M. Huang, H. Liu, X.
Feng, Z. Lin, W. Zhang, W.-B. Zhang and S. Z. D. Cheng, *Polymer*,
2017, **125**, 303-329.
 35. R. Nagarajan, *Langmuir*, 2002, **18**, 31-38.
 36. K. Wu, M. Huang, K. Yue, C. Liu, Z. Lin, H. Liu, W. Zhang, C.-H.
Hsu, A.-C. Shi, W.-B. Zhang and S. Z. D. Cheng, *Macromolecules*,
2014, **47**, 4622-4633.
 37. L. Cui, J. P. Collet, G. Xu and L. Zhu, *Chem. Mater.*, 2006, **18**,
3503-3512.
 38. M. Huang, C.-H. Hsu, J. Wang, S. Mei, X. Dong, Y. Li, M. Li, H. Liu,
W. Zhang, T. Aida, W.-B. Zhang, K. Yue and S. Z. D. Cheng,
Science, 2015, **348**, 424-428.
 39. H. Liu, J. Luo, W. Shan, D. Guo, J. Wang, C.-H. Hsu, M. Huang, W.
Zhang, B. Lotz, W.-B. Zhang, T. Liu, K. Yue and S. Z. D. Cheng,
ACS Nano, 2016, **10**, 6585-6596.
 40. J. Zhang, L.-Q. Wang, H. Wang and K. Tu, *Biomacromolecules*,
2006, **7**, 2492-2500.
 41. A. J. Waddon and E. B. Coughlin, *Chem. Mater.*, 2003, **15**, 4555-
4561.

